Speckle Reduction in Images with WEAD and WECD

Jeny Rajan[1] and M.R. Kaimal[2]

[1] NeST, Technopark, Trivandrum, India
[2] Department of Computer Science, University of Kerala, Trivandrum, India
jenyrajan@rediffmail.com, mrkaimal@yahoo.com

Abstract. In this paper we discuss the speckle reduction in images with the recently proposed Wavelet Embedded Anisotropic Diffusion (WEAD) and Wavelet Embedded Complex Diffusion (WECD). Both these methods are improvements over anisotropic and complex diffusion by adding wavelet based bayes shrink in its second stage. Both WEAD and WECD produces excellent results when compared with the existing speckle reduction filters. The comparative analysis with other methods were mainly done on the basis of Structural Similarity Index Matrix (SSIM) and Peak Signal to Noise Ratio (PSNR). The visual appearance of the image is also considered.

1 Introduction

Speckle noise is a common phenomenon in all coherent imaging systems like laser, acoustic, SAR and medical ultrasound imagery [1]. For images that contain speckle, the goal of enhancement is to remove the speckle without destroying important image features [2]. Synthetic Aperture Radar (SAR) images are corrupted by speckle noise due to the interference between waves reflected from microscopic scattering through the terrain. Because of its undesirable effect, speckle noise reduction turns out to be a key pre-processing step in order to interpret SAR images efficiently [3]. In medical imaging, the grainy appearance of 2D ultrasound images is due mainly to speckle. Here the speckle phenomenon results from the constructive-destructive interference of the coherent ultrasound pulses back scattered from the tiny multiple reflector that constitute biological materials. Speckle typically has the unfortunate aspect of falling into the high sensitivity region of human vision to spatial frequency. The frequency spectrum of speckle is also similar to the imaging system modulation transfer function. Speckle can therefore obscure the diagnostically important information.[4]. In certain applications, however the removal of speckle may be counter productive. Examples in which speckle preservation is important include feature tracking in ultrasonic imaging [5] and detection of features that are the same scale as the speckle patterns (e.g., coagulation damage) [6]. The source of speckle noise is attributed to random interference between the coherent returns. Fully developed speckle noise has the characteristic of multiplicative noise [7]. Speckle noise follows a gamma distribution and is given as

P. Kalra and S. Peleg (Eds.): ICVGIP 2006, LNCS 4338, pp. 184 – 193, 2006.

$$F(g)=\frac{g^{\alpha-1}}{(\alpha-1)!a^{\alpha}}e^{\frac{-g}{a}} \tag{1}$$

where g is the gray level and α is the variance. Below figure shows the plot of speckle noise distribution.

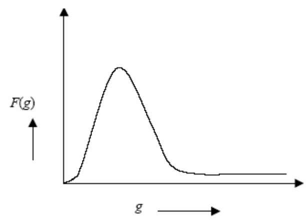

Fig. 1. Plot of speckle noise distribution

A number of methods are proposed in the literature for removing speckle from ultrasound images. Popular methods among them are Lee, Frost, Kuan, Gamma and SRAD filters. The Lee and Kuan filters have the same formation, although the signal model assumptions and the derivations are different. Essentially, both the Lee and Kuan filters form an output image by computing a linear combination of the center pixel intensity in a filter window with the average intensity of the window. So, the filter achieves a balance between straightforward averaging (in homogeneous regions) and the identity filter (where edges and point features exist). This balance depends on the coefficient of variation inside the moving window[2].

The Frost filter also strikes a balance between averaging and the all-pass filter. In this case, the balance is achieved by forming an exponentially shaped filter kernel that can vary from a basic average filter to an identity filter on a point wise, adaptive basis. Again, the response of the filter varies locally with the coefficient of variation. In case of low coefficient of variation, the filter is more average-like, and in cases of high coefficient of variation, the filter attempts to preserve sharp features by not averaging. The Gamma filter is a Maximum A Posteriori (MAP) filter based on a Bayesian analysis of the image statistics [1]. Speckle Reducing Anisotropic Diffusion (SRAD) is an edge sensitive diffusion method for speckled images [2].

Wavelet Embedded Anisotropic Diffusion (WEAD) [8] and Wavelet Embedded Complex Diffusion (WECD)[9] are extensions of non linear Anisotropic and Complex diffusion by adding Bayesian shrinkage at its second stage. The methods increase the speed of processing and improve the quality of images than their parent methods.

The paper is organized as follows. Section 2 deals with diffusion techniques for removing noise from images. It mainly discusses anisotropic and complex diffusion. Section 3 explains the recently proposed WEAD and WECD and its capability to remove speckle noises. Experimental results and comparative analysis with other popular methods is shown in Section 4. Finally conclusion and remarks are added in Section 5.

2 Noise Removal with Diffusion Techniques

Diffusion is a physical process that equilibrates concentration differences without creating or destroying mass [10]. This physical observation, the equilibrium property can be expressed by Fick's law

$$j = -D.\nabla u \tag{2}$$

This equation states that a concentration gradient ∇u causes a flux j, which aims to compensate for this gradient. The relation between ∇u and j is described by the diffusion tensor D, a positive definite symmetric matrix. The case where j and ∇u are parallel is called isotropic. Then we may replace the diffusion tensor by a positive scalar valued diffusivity g. In the general case i.e., anisotropic case, j and ∇u are not parallel. The observation that diffusion does only transport mass without destroying it or creating new mass is expressed by the continuity equation

$$d_t u = -\text{div } j \tag{3}$$

where t denotes the time. If we apply the Fick's law into the continuity equation we will get the diffusion equation. i.e.,

$$\frac{\partial u}{\partial t} = Div(D \cdot \nabla u) \tag{4}$$

This equation appears in many physical transport process. In the context of heat transfer, it is called the heat equation [10]. When applied to an image, the linear diffusion will generate scale space images. Each image will be more smoothed than the previous one. By smoothing an image, to some extend noise can be removed. This is why linear diffusion is used for noise removal. But one problem with this method is its inability to preserve image structures.

2.1 Anisotropic Diffusion

To avoid the defects of linear diffusion (especially the inability to preserve edges and to impel inter region smoothing before intra region smoothing) non-linear partial differential equations can be used. In [11] Perona and Malik has given 3 necessary conditions for generating multiscale *semantically meaningful* images

1. Causality : Scale space representation should have the property that no spurious detail should be generated passing from finer to coarser scale.
2. Immediate Localization : At each resolution, the region boundaries should be sharp and coincide with the semantically meaningful boundaries at that resolution.
3. Piecewise Smoothing : At all scales, intra region smoothing should occur preferentially over inter region smoothing.

Linear diffusion is especially not satisfying the third condition, which can be overcome by using a non linear one. Among the non linear diffusion , the one proposed by

Perona and Malik [11] and its variants are the most popular. They proposed a nonlinear diffusion method for avoiding the blurring and localization problems of linear diffusion filtering. There has been a great deal of interest in this anisotropic diffusion as a useful tool for multiscale description of images, image segmentation, edge detection and image enhancement [12]. The basic idea behind anisotropic diffusion is to evolve from an original image $u_0(x, y)$, defined in a convex domain $\Omega \subset R \times R$, a family of increasingly smooth images $u(x,y,t)$ derived from the solution of the following partial differential equation [11] :

$$\frac{\partial u}{\partial t} = div\left[c(\nabla u)\nabla u\right] \quad ,u(x, y)\big|_{t=0} = u_0(x, y) \tag{5}$$

where ∇u is the gradient of the image *u*, *div* is the divergence operator and c is the diffusion coefficient. The desirable diffusion coefficient *c(.)* should be such that equation (5) diffuses more in smooth areas and less around less intensity transitions, so that small variations in image intensity such as noise and unwanted texture are smoothed and edges are preserved. Another objective for the selection of *c(.)* is to incur backward diffusion around intensity transitions so that edges are sharpened, and to assure forward diffusion in smooth areas for noise removal [12]. Here are some of the previously employed diffusivity functions[13] :

A. Linear diffusivity [14]:

$$c(s) = 1, \tag{6}$$

B. Charbonnier diffusivity [15]:

$$c(s) = \frac{1}{\sqrt{1 + \frac{s^2}{k^2}}} \tag{7}$$

C. Perona−Malik diffusivity [11] :

$$c(s) = \frac{1}{1 + \left(\frac{s}{k}\right)^2} \tag{8}$$

$$c(s) = \exp\left[-\left(\frac{s}{k}\right)^2\right] \tag{9}$$

D. Weickert diffusivity[10] :

$$c(s) = \begin{cases} 1 & s = 0 \\ 1 - \exp\left(\dfrac{-3.31488}{\left(s/k\right)^8}\right) & s > 0 \end{cases} \tag{10}$$

E. TV diffusivity [16] :

$$c(s) = \frac{1}{s} \tag{11}$$

F. BFB diffusivity [17]:

$$c(s) = \frac{1}{s^2} \tag{12}$$

2.2 Complex Diffusion

In 1931 Schrodinger explored the possibility that one might use diffusion theory as a starting point for the derivation of the equations of quantum theory. These ideas were developed by *Fuerth* who indicated that the Schrodinger equation could be derived from the diffusion equation by introducing a relation between the diffusion coefficient and Planck's constant, and stipulating that the probability amplitude of quantum theory should be given by the resulting differential equation [18]. It has been the goal of a variety of subsequent approaches to derive the probabilistic equations of quantum mechanics from equations involving probabilistic or stochastic processes. The time dependent Schrodinger equation is the fundamental equation of quantum mechanics. In the simplest case for a particle without spin in an external field it has the form [19]

$$i\hbar\frac{\partial\psi}{\partial t} = -\frac{\hbar^2}{2m}\Delta\psi + V(x)\psi \tag{13}$$

where $\psi = \psi(t,x)$ is the wave function of a quantum particle, m is the mass of the particle, $\hbar$ is Planck's constant, $V(x)$ is the external field potential, Δ is the Laplacian and $i = \sqrt{-1}$. With an initial condition $\psi|_{t=0} = \psi_0(x)$, requiring that $\psi(t,\cdot) \in L_2$ for each fixed t, the solution is $\psi(t,\cdot) = e^{\frac{-i}{h}tH}\psi_0$, where the exponent is shorthand for the corresponding power series, and the higher order terms are defined recursively by $H^n\psi = H\left(H^{n-1}\psi\right)$. The operator

$$H = -\frac{\hbar^2}{2m}\Delta + V(x) \tag{14}$$

called the Schrodinger operator, is interpreted as the energy operator of the particle under consideration. The first term is the kinetic energy and the second is the potential energy. The duality relations that exist between the Schrodinger equation and the diffusion theory have been studied in [9]. The standard linear diffusion equation is as in (4). From (13) and (4) we can derive the following two equations.

$$I_{RT} = C_R I_{Rxx} - C_I I_{Ixx} \; , I_{R|t=0} = I_0 \tag{15}$$

$$I_{IT} = C_I I_{Rxx} + C_R I_{Ixx} \; , I_{I|t=0} = 0 \tag{16}$$

where I_{RT} is the image obtained at real plane and I_{IT} is the image obtained at imaginary plane at time T and $C_R = \cos(\theta)$, $C_I = \sin(\theta)$. The relation $I_{Rxx} >> \theta I_{Ixx}$ holds for small theta approximation[8]:

$$I_{RT} \approx I_{Rxx}; \qquad I_{It} \approx I_{Ixx} + \theta I_{Rxx} \tag{17}$$

In (17) I_R is controlled by a linear forward diffusion equation, whereas I_I is affected by both the real and imaginary equations. The above said method is linear complex diffusion equation.

A more efficient nonlinear complex diffusion can be written as in eqn. (18) [19]

$$I_t = \nabla \cdot (c(\mathrm{Im}(I)\nabla I) \tag{18}$$

where

$$c(\mathrm{Im}(I)) = \frac{e^{i\theta}}{1+\left(\frac{\mathrm{Im}(I)}{k\theta}\right)^2} \tag{19}$$

where k is the threshold parameter Non linear complex diffusion seems to be more efficient than linear complex diffusion in terms of preserving edges.

3 WEAD and WECD

Both WEAD and WECD are improvements of anisotropic and complex diffusion by adding BayesShrink [20] at the second stage. In the case of WEAD, Bayesian Shrinkage of the non-linearly diffused signal is taken. The equation can be written as

$$I_n = B_s(I'_{n-1}) \tag{20}$$

and in the case of WECD the Bayesian Shrinkage of the real part of the non-linearly complex diffused signal is taken. The equation can be written as

$$I_n = B_s(R_c(I'_{n-1})) \tag{21}$$

where B_s is the bayesian shrink and I'_{n-1} is anisotropic diffusion as shown in (5) at (n-1)th time and $R_c(I'_{n-1})$ is the real part of the non linearly diffused complex diffusion.

Numerically (20) and (21) can be written as

$$I_n = B_s\left(I_{n-1} + \Delta t d_n\right) \tag{22}$$

and

$$I_n = B_s(R_c(I_{n-1} + \Delta t d_n)) \tag{23}$$

respectively.

The intention behind these two methods is to decrease the convergence time of the anisotropic diffusion and complex diffusion respectively. It is understood that the convergence time for denoising is directionally proportional to the image noise level. In the case of diffusion, as iteration continues, the noise level in image decreases (till it reaches the convergence point), but in a slow manner. But in the case of Bayesian Shrinkage, it just cut the frequencies above the threshold and that in a single step. An iterative Bayesian Shrinkage will not incur any change in the detail coefficients from

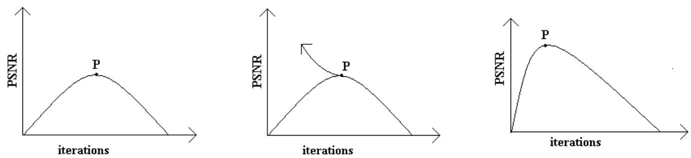

(a) (b) (c)

Fig. 2. Working of WEAD & WECD (a) Shows the convergence of a noisy image (convergence at P). If this P can be shifted towards left, image quality can be increased and time complexity can be reduced. Illustrated in (b). (c) shows the signal processed by WEAD & WECD. It can be seen that the convergence point is shifted to left and moved upwards.

the first one. Now consider the case of WEAD and WECD, here the threshold for Bayesian shrinkage is recalculated each time after diffusion, and since as a result of two successive noise reduction step, it approaches the convergence point much faster than anisotropic diffusion or complex diffusion.

As the convergence time decreases, image blurring can be restricted, and as a result image quality increases. The whole process is illustrated in Fig. 2. Fig. 2(a) shows the convergence of the image processed by diffusion methods. The convergence point is at **P**. i.e. at **P** we will get the better image, with the assumption that the input image is a noisy one. If this convergence point **P** can be shifted towards y-axis, its movement will be as in the figure shown in Fig 2 (b).i.e. if we pull the point **P** towards y-axis, it will move in a left-top fashion. Here the Bayesian shrinkage is the catalyst, which pulls the convergence point **P** of the anisotropic or complex diffusion towards a better place.

4 Experimental Results and Comparative Analysis

Experiments were carried out on various types of standard images. Comparisons and analysis were done on the basis of MSSIM (Mean Structural Similarity Index Matrix) [21] and PSNR (Peak Signal to Noise Ratio). SSIM is used to evaluate the overall image quality and is in the range 0 to 1. The SSIM works as follows, suppose x and y be two non negative image signals, one of the signals to have perfect quality, then the similarity measure can serve as a quantitative measure of the quality of the second signal. The system separates the task of similarity measurement into three comparisons: luminance, contrast and structure. The PSNR is given in decibel units (dB), which measure the ratio of the peak signal and the difference between two images.

Fig.3 shows the performance of various filters against speckle noise. It can be seen that the image processed by WEAD and WECD given a better result than the other three speckle filters. Table 1 shows a comparative analysis of popular speckle filters with WEAD and WECD. Various levels of noise are added to image for testing its capability. In all the cases the performance of WEAD and WECD was superior to others.

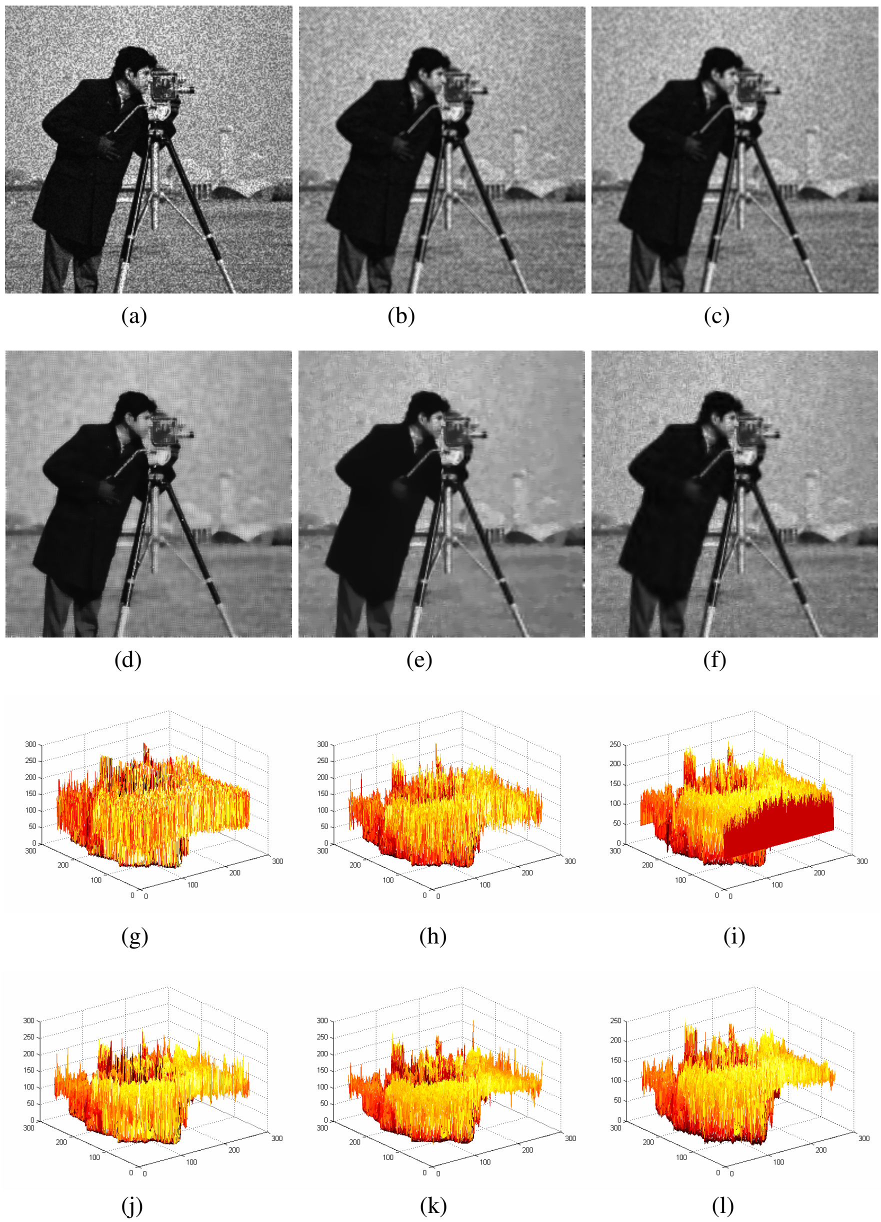

Fig. 3. Speckle affected image processed with various filters (a) Image with speckle noise (PSNR 18.85), (b) Image processed with Frost Filter (PSNR : 22.37), (c) Image Processed with Kuan Filter (PSNR : 23.12), (d) Image processed with SRAD (PSNR: 23.91), (e) Image processed with WEAD (PSNR : 25.40), (f) Image Processed with WECD (PSNR :24.52), (g), (h),(i), (j),(k),(l) shows the 3D plot of (a),(b),(c),(d),(e),(f)

Table 1. Comparative analysis of various speckle filters

Method	PSNR	MSSIM	Time Taken (in seconds)
Image : Cameraman, Noise variance : 0.04, PSNR : 18.85, MSSIM : 0.4311			
Frost	22.37	0.4885	5.75
Kuan	23.12	0.5846	10.00
SRAD	23.91	0.5923	0.68
WEAD	25.40	0.6835	31.00
WECD	24.52	0.6092	7.23
Image : Lena, Noise variance : 0.02 , PSNR : 24.16, MSSIM : 0.6047			
Frost	26.77	0.7027	5.81
Kuan	25.59	0.7916	9.96
SRAD	27.42	0.7750	0.75
WEAD	29.08	0.8208	18.56
WECD	28.56	0.7941	3.48
Image : Bird, Noise variance : 0.04, PSNR : 18.66 , MSSIM : 0.2421			
Frost	24.2604	0.4221	5.84
Kuan	25.78	0.5817	10.00
SRAD	27.65	0.6792	0.99
WEAD	29.98	0.8318	49.45
WECD	28.38	0.7117	17.59

5 Conclusion

In this paper a comparative analysis of Wavelet Embedded Anisotropic Diffusion (WEAD) and Wavelet Embedded Complex Diffusion (WECD) with other methods is done. When compared with other methods it can be seen that the complexity and processing time of WEAD and WECD is slightly more but the performance is superior. The hybrid concept used in WEAD and WECD can be extended to other PDE based methods.

References

1. L Gagnon, A Jouan, Speckle Filtering of SAR Images – A Comparative Study between Complex-Wavelet-Based and Standard Filters, Wavelet Applications in Signal and Image Processing : Proceedings of SPIE, Vol. 3169, (1997) 80-91
2. Yongjian Yu, Scott T Acton, Speckle Reducing Anisotropic Diffusion, IEEE Trans. on Image Processing, Vol. 11 (2002) 1260–1270
3. Zhao Hui Zhang, Veronique Prinet, SongDe MA, A New Method for SAR Speckle Reduction, IEEE (2002)
4. R.N Rohling, A.H. Gee, Issues in 3-D Free-Hand Medical Ultrasound Imaging, Technical Report, Cambridge University Engineering Department (1996)

5. G.E Trahey, S.M. Hubbard, O.T von Ramm, Angle Independent Ultrasonic Blood Flow Dtection by Frame-to-Frame Correlation of B-mode Images, Ultrasonics, Vol 26, (1988) 271 – 276
6. Z. Sun, H. Ying, J. Lu, A Noninvasive Cross-Correlation Ultrasound Technique for Detecting Spatial Profile of Laser – Induced Coagulation Damage – An *in vitro* Study, IEEE Trans. on Biomed. Engg., Vol. 48, (2001) 223-229
7. Sarita Dangeti, Denoising Techniques – A Comparison, Thesis Report, Submitted to the Dept. of Electrical and Computer Engineering, Louisiana State University and Agricultural and Mechanical College, (2003)
8. Jeny Rajan, M.R. Kaimal, Image Denoising using Wavelet Embedded Anisotropic Diffusion (WEAD), Proceedings of IEE International Conference on Visual Information Engineering, (2006)
9. Jeny Rajan, Image Denoising using Partial Differential Equations, M.Tech. Thesis, Submitted to Department of Computer Science, University of Kerala (INDIA), (2005).
10. Joachim Weickert, Anisotropic Diffusion in Image Processing, ECMI Series, Teubner – Verlag (1998)
11. P. Perona, J. Malik, Scale Space and Edge Detection using Anisotropic Diffusion, IEEE Trans. on Pattern Analysis and Machine Intelligence, Vol. 12. (1990) 629-639
12. Yu-Li You, Wenguan Xu, Allen Tannenbaum, Mostafa Kaveh, Behavioral Analysis of Analysis of Anisotropic Diffusion, IEEE Trans. on Image Processing, Vol. 5, (1996)
13. Pavel Mrazek, Joachim Weickert, Gabriele Steidl, Correspondence between Wavelet Shrinkage and Non linear Diffusion, Scale Space 2003, LNCS 2695, (2003) 101-116
14. T. Lijima, Basic Theory on Normalization of Pattern, Bulletin of the Electrotechnical Laboratory, Vol. 26, (1962) 368-388
15. P. Charbonnier, G. Aubert, L. Blanc-Feraud and M. Barlaud, Two deterministic half-quadratic regularization algorithms for computed imaging, In Proc. 1994 IEEE International Conference on Image Processing, Vol. 2, (1994) 168–172
16. F. Andreu, C. Ballester, V. Caselles, and J. M. Mazn, Minimizing total variation flow, Differential and Integral Equations, Vol 14, (2001) 321 – 360
17. S. L. Keeling and R. Stollberger, Nonlinear anisotropic diffusion filters for wide range edge sharpening, Inverse Problems, Vol 18, (2002) 175-190
18. M.D. Kostin, Schrodinger-Fuerth quantum diffusion theory: Generalized complex diffusion equation, J. Math. Phys, (1992)
19. Guy Gilboa, Nir Sochen and Yehoshua Y Zeevi, Image Enhancement and Denoising by Complex Diffusion Processes, IEEE Trans. On Pattern Analysis and Machine Imtelligence, Vol. 26, (2004).
20. S. Grace Chang, Bin Yu and Martin Vetterli, Adaptive Wavelet Thresholding for Image Denoising and Compression, IEEE Trans. Image Processing, Vol 9, (2000)
21. Zhou Wang, Alan Conard Bovik, Hamid Rahim Sheik and Erno P Simoncelli, Image Quality Assessment : From Error Visibility to Structural Similarity, IEEE Trans. Image Processing, Vol. 13, (2004)